

# Cosmological Implications of X-ray Clusters of Galaxies

Yasushi Suto and Tetsu Kitayama

*Department of Physics and Research Center for the Early Universe  
The University of Tokyo, Tokyo 113-0033, Japan*

Shin Sasaki

*Department of Physics, Tokyo Metropolitan University, Hachioji  
Tokyo 192-0364, Japan*

**Abstract.** Cosmological implications of clusters of galaxies are discussed with particular attention to their importance in probing the cosmological parameters. More specifically we compute the number counts of clusters of galaxies,  $\text{Log}N\text{-Log}S$  relation, in X-ray and submm bands on the basis of the Press-Schechter theory. We pay particular attention to a set of theoretical models which well reproduce the *ROSAT* 0.5-2 keV band  $\text{Log}N\text{-Log}S$ , and explore possibilities to break the degeneracy among the viable cosmological models.

## 1. Introduction

There are several reasons why clusters of galaxies are regarded as useful probes of cosmology including (i) since dynamical time-scale of clusters is comparable to the age of the universe, they should retain the cosmological initial condition fairly faithfully. (ii) clusters can be observed in various bands including optical, X-ray, radio, mm and submm bands, and in fact recent and future big projects (e.g., SDSS, AXAF, PLANCK) aim to make extensive surveys and detailed imaging/spectroscopic observations of clusters. (iii) to the first order, clusters are well approximated as a system of dark matter, gas and galaxies, and thus theoretically well-defined and relatively well-understood, at least compared with galaxies themselves, and (iv) on average one can observe a higher- $z$  universe with clusters than with galaxies. In particular X-ray observations are well-suited for the study of clusters since the X-ray emissivity is proportional to  $n_e^2$  and thus less sensitive to the projection contamination which has been known to be a serious problem in their identifications with the optical data.

In fact, various statistics related to the abundances of clusters has been extensively studied to constrain theories of structure formation, including mass function (Bahcall & Cen 1993; Ueda, Itoh, & Suto 1993), velocity function (Shimasaku 1993; Ueda, Shimasaku, Suginoara, & Suto 1994), X-ray Temperature function (hereafter XTF, Henry & Arnaud 1991; White, Efstathiou, & Frenk 1993; Kitayama & Suto 1996; Viana & Liddle 1996; Eke, Cole, & Frenk 1996; Pen 1996). Previous authors have focused on cosmological implications of cluster XTF mainly because theoretical predictions are relatively easier although

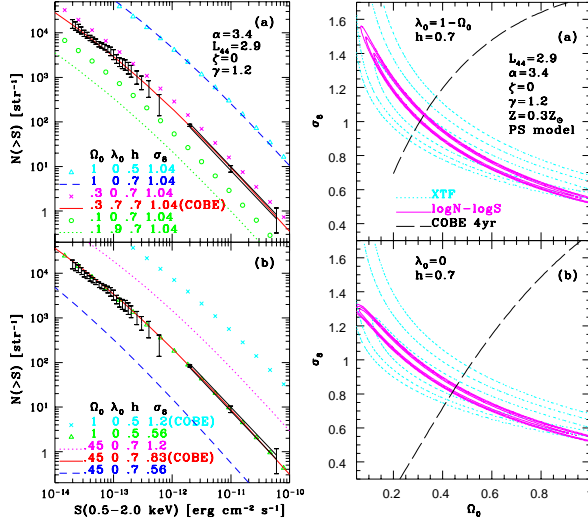


Figure 1. *Left:* Theoretical predictions for  $\text{Log}N\text{-Log}S$  of X-ray clusters in CDM models with different cosmological parameters; (a)  $\sigma_8 = 1.04$  models with different  $\Omega_0$ ,  $\lambda_0$  and  $h$ , (b)  $\Omega_0 = 1$  and  $0.45$  models with different  $\sigma_8$ . Denoted by (COBE) are the models normalized according to the *COBE* 4 year data (Bunn & White 1997). Data points with error bars at  $S \lesssim 10^{-12}$  erg cm $^{-2}$  s $^{-1}$  are from the *ROSAT* Deep Cluster Survey (RDCS, Rosati et al. 1995; Rosati & Della Ceca 1997), and the error box at  $S \gtrsim 2 \times 10^{-12}$  represents a power-law fitted region from the *ROSAT* Brightest Cluster Sample (BCS, Ebeling et al. 1997). For the BCS data at  $S = 2 \times 10^{-12}$ ,  $1 \times 10^{-11}$  and  $6 \times 10^{-11}$  erg cm $^{-2}$  s $^{-1}$ , we also plot the corresponding Poisson errors. *Right:* Limits on  $\Omega_0$  and  $\sigma_8$  in CDM models ( $n = 1$ ,  $h = 0.7$ ) with (a)  $\lambda_0 = 1 - \Omega_0$ , and (b)  $\lambda_0 = 0$ . Constraints from cluster  $\text{Log}N\text{-Log}S$  (solid) and XTF (dotted) are plotted as contours at  $1\sigma$  (68%),  $2\sigma$  (95%) and  $3\sigma$  (99.7%) confidence levels. Dashed lines indicate the *COBE* 4 year results from Bunn & White (1997).

the observational data are statistically limited. In addition, the conversion to the number density at high  $z$  becomes very sensitive to the adopted cosmological parameters. On the other hand,  $\text{Log}N\text{-Log}S$  which we discuss in details below is observationally more robust (Ebeling et al. 1997; Rosati & Della Ceca 1997) while its theoretical prediction is more model-dependent (Oukbir, Bartlett, & Blanchard 1996; Kitayama & Suto 1997; Kitayama, Sasaki & Suto 1998). In this respect, both statistics are complementary.

## 2. $\text{Log} N - \text{Log} S$ of X-ray clusters

We compute the number of clusters observed per unit solid angle with X-ray flux greater than  $S$  by

$$N(> S) = \int_0^\infty dz d_A^2(z) c \left| \frac{dt}{dz} \right| \int_S^\infty dS (1+z)^3 n_M(M, z) \frac{dM}{dT_{\text{gas}}} \frac{dT_{\text{gas}}}{dL_{\text{band}}} \frac{dL_{\text{band}}}{dS}, \quad (1)$$

where  $c$  is the speed of light,  $t$  is the cosmic time,  $d_A$  is the angular diameter distance,  $T_{\text{gas}}$  and  $L_{\text{band}}$  are respectively the gas temperature and the band-limited absolute luminosity of clusters, and  $n_M(M, z)dM$  is the comoving number density of virialized clusters of mass  $M \sim M + dM$  at redshift  $z$ .

Given the observed flux  $S$  in an X-ray energy band  $[E_a, E_b]$ , the source luminosity  $L_{\text{band}}$  at  $z$  in the corresponding band  $[E_a(1+z), E_b(1+z)]$  is written as

$$L_{\text{band}}[E_a(1+z), E_b(1+z)] = 4\pi d_L^2(z)S[E_a, E_b], \quad (2)$$

where  $d_L = (1+z)^2 d_A$  is the luminosity distance. We adopt the observed  $L_{\text{bol}} - T_{\text{gas}}$  relation parameterized by

$$L_{\text{bol}} = L_{44} \left( \frac{T_{\text{gas}}}{6\text{keV}} \right)^\alpha (1+z)^\zeta 10^{44} h^{-2} \text{ erg sec}^{-1}. \quad (3)$$

We take  $L_{44} = 2.9$ ,  $\alpha = 3.4$  and  $\zeta = 0$  as a fiducial set of parameters on the basis of recent observational indications (David et al. 1993; Ebeling et al. 1996; Ponman et al. 1996; Mushotzky & Scharf 1997). Then we translate  $L_{\text{bol}}(T_{\text{gas}})$  into the band-limited luminosity  $L_{\text{band}}[T_{\text{gas}}, E_1, E_2]$  by properly taking account of metal line emissions (Masai 1984) in addition to the thermal bremsstrahlung (we fix the abundance of intracluster gas as 0.3 times the solar value).

Assuming that the intracluster gas is isothermal, its temperature  $T_{\text{gas}}$  is related to the total mass  $M$  by

$$\begin{aligned} k_B T_{\text{gas}} &= \gamma \frac{\mu m_p G M}{3 r_{\text{vir}}(M, z_f)}, \\ &= 5.2\gamma(1+z_f) \left( \frac{\Delta_{\text{vir}}}{18\pi^2} \right)^{1/3} \left( \frac{M}{10^{15} h^{-1} M_\odot} \right)^{2/3} \Omega_0^{1/3} \text{ keV}. \end{aligned} \quad (4)$$

where  $k_B$  is the Boltzmann constant,  $G$  is the gravitational constant,  $m_p$  is the proton mass,  $\mu$  is the mean molecular weight (we adopt  $\mu = 0.59$ ), and  $\gamma$  is a fudge factor of order unity which may be calibrated from hydrodynamical simulations or observations. The virial radius  $r_{\text{vir}}(M, z_f)$  of a cluster of mass  $M$  virialized at  $z_f$  is computed from  $\Delta_{\text{vir}}$ , the ratio of the mean cluster density to the mean density of the universe at that epoch. We evaluate this quantity using the formulae for the spherical collapse model presented in Kitayama & Suto (1996b) and assuming for simplicity that  $z_f$  is equal to the epoch  $z$  at which the cluster is observed. Finally, we compute the mass function  $n_M(M, z)dM$  in equation (1) using the Press-Schechter theory (Press & Schechter 1974) assuming  $z = z_f$  as above. The effect of  $z_f \neq z$  is discussed by Kitayama & Suto (1997) in this context, and the more general consideration of  $z_f \neq z$  is given in Lacey & Cole (1993), Sasaki (1994), and Kitayama & Suto (1996a,b).

### 3. Breaking the degeneracy

The X-ray  $\text{Log}N - \text{Log}S$  for various Cold Dark Matter (CDM) models and the resulting constraints on  $\Omega_0$  and  $\sigma_8$  are summarized in Fig.1. Figure 1 presents a clear example of the degeneracy among viable cosmological models in a sense that for a given value of  $\Omega_0$ , one can find a value of  $\sigma_8$  which accounts for the

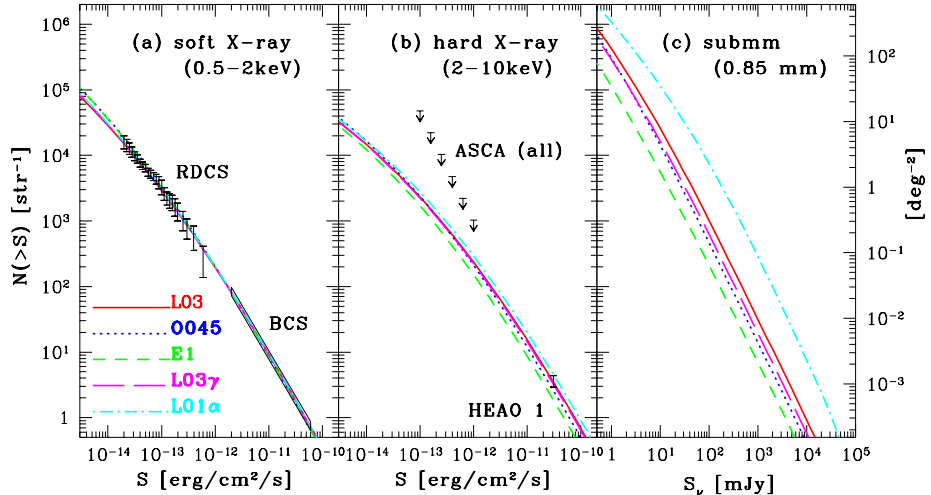


Figure 2. The  $\text{Log}N$ – $\text{Log}S$  relations of galaxy clusters for CDM models in (a) the soft X-ray (0.5–2.0 keV) band, (b) the hard X-ray (2–10 keV) band, and (c) the submm (0.85 mm) band. Lines represent the models listed in table 1; L03 (solid), O045 (dotted), E1 (short dashed), L03 $\gamma$  (long dashed), and L01 $\alpha$  (dot-dashed). Also plotted in panel (a) are the  $1\sigma$  error bars from the RDCS (Rosati et al. 1995, 1997), and the error box from the BCS (Ebeling et al. 1997). In panel (b), the arrows indicate the  $\text{Log}N$ – $\text{Log}S$  of all X-ray sources in the 2–10 keV band from *ASCA* (Cagnoni et al. 1997), and the error bar ( $1\sigma$ ) is the number of clusters observed by *HEAO 1* (Piccinotti et al. 1982).

X-ray cluster  $\text{Log}N$ – $\text{Log}S$ . Several examples of such models are listed in Table 1.

Table 1. CDM models from the *ROSAT* X-ray  $\text{Log}N$  –  $\text{Log}S$ .

| Model        | $\Omega_0$ | $\lambda_0$ | $h$ | $\sigma_8$ | $\alpha$ | $\gamma$ |
|--------------|------------|-------------|-----|------------|----------|----------|
| L03          | 0.3        | 0.7         | 0.7 | 1.04       | 3.4      | 1.2      |
| O045         | 0.45       | 0           | 0.7 | 0.83       | 3.4      | 1.2      |
| E1           | 1.0        | 0           | 0.5 | 0.56       | 3.4      | 1.2      |
| L03 $\gamma$ | 0.3        | 0.7         | 0.7 | 0.90       | 3.4      | 1.5      |
| L01 $\alpha$ | 0.1        | 0.9         | 0.7 | 1.47       | 2.7      | 1.2      |

The degeneracy among viable cosmological models can be broken by observing wider (i.e., increase the statistics using wide-field surveys like SDSS, 2dF, PLANCK) and deeper (at higher redshifts) in different bands. (e.g., Eke, Cole, & Frenk 1996; Barbosa, Bartlett, Blanchard, & Oukbir 1996; Fan, Bahcall, & Cen 1997; Kitayama, Sasaki, & Suto 1998). Figure 2 plots the cluster  $\text{Log}N$ – $\text{Log}S$  predictions in soft-Xray, hard X-ray, and submm (due to the Sunyaev-Zel’dovich effect) for models which reproduce the observed  $\text{Log}N$ – $\text{Log}S$  in the

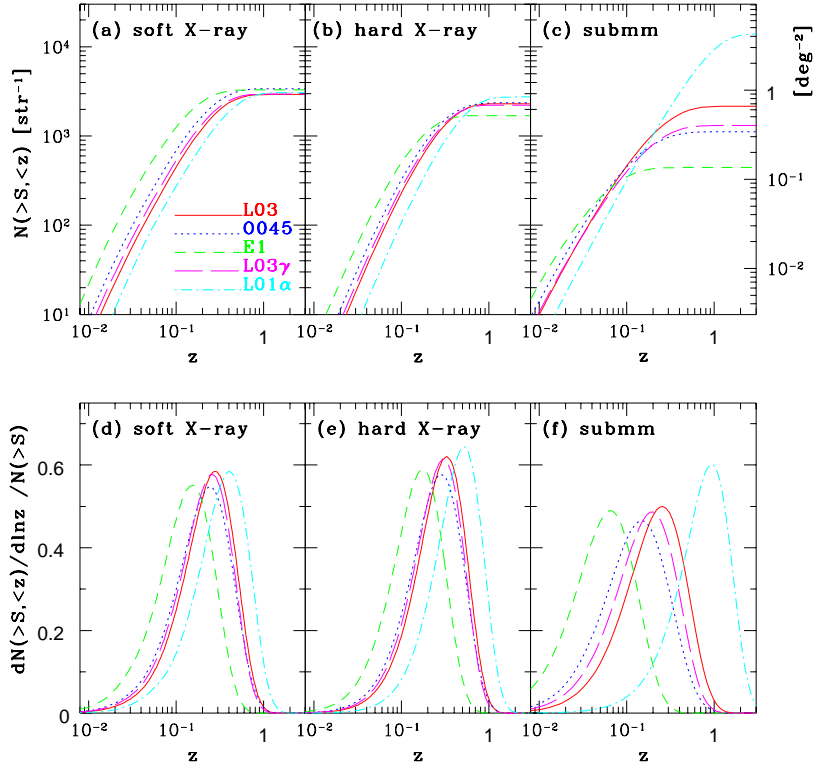


Figure 3. Redshift evolution of the number of galaxy clusters. Upper panels show the cumulative number  $N(> S, < z)$  against  $z$  in (a) the soft X-ray (0.5-2 keV) band with  $S = 10^{-13}$  erg cm $^{-2}$  s $^{-1}$ , (b) the hard X-ray (2-10 keV) band with  $S = 10^{-13}$  erg cm $^{-2}$  s $^{-1}$ , and (c) the submm (0.85 mm) band with  $S_\nu = 50$  mJy. Lower panels (d)–(f) are similar to (a)–(c) except for plotting the differential distribution  $dN(> S, < z)/d \ln z$  normalized by  $N(> S)$ .

soft-Xray band (Table 1). Figure 4 illustrates the extent to which one can break the degeneracy between  $\sigma_8$  and  $\Omega_0$  in CDM models ( $n = 1$ ,  $h = 0.7$ ) using the multi-band observational data.

Similarly the redshift-distribution of cluster abundances can be a very powerful discriminator of the different cosmological models. Figure 3 exhibits the redshift evolution of the number of clusters in different bands. As expected, the evolutionary behavior strongly depends on the values of  $\Omega_0$  and  $\sigma_8$ ; the fraction of low redshift clusters becomes larger for greater  $\Omega_0$  and smaller  $\sigma_8$ . It is indicated that one may be able to distinguish among these models merely by determining the redshifts of clusters up to  $z \sim 0.2$ . For this purpose, we adopt tentatively the X-ray brightest Abell-type clusters (XBACs, Ebeling et al. 1996), which is about 80 % complete and consists of 242 clusters with  $S > 5 \times 10^{-12}$  erg cm $^{-2}$  s $^{-1}$  in the 0.1-2.4 keV band and  $z < 0.2$ . Keeping in mind the incompleteness of the sample and uncertainties especially in the estimated temperature

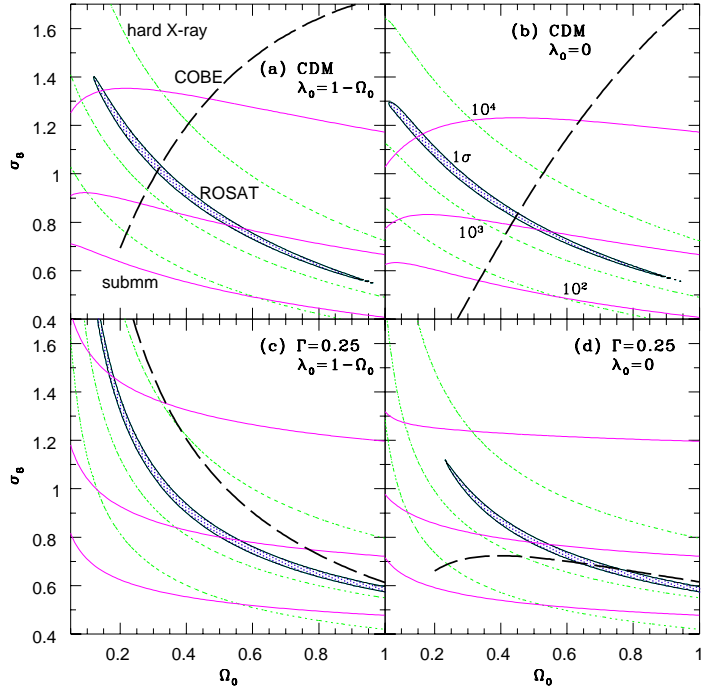


Figure 4. Contour maps on the  $\Omega_0$ - $\sigma_8$  plane in (a) spatially flat ( $\lambda_0 = 1 - \Omega_0$ ) CDM models, (b) open ( $\lambda_0 = 0$ ) CDM models, (c) spatially flat CDM-like models with the fixed shape parameter ( $\Gamma = 0.25$ ), and (d) open CDM-like models with  $\Gamma = 0.25$ . In all cases,  $h = 0.7$ ,  $\alpha = 3.4$ , and  $\gamma = 1.2$  are assumed. Shaded regions represent the  $1\sigma$  significance contours derived in KS97 from the soft X-ray (0.5-2 keV)  $\text{Log}N$ - $\text{Log}S$ . Dotted and solid lines indicate the contours of the number of clusters greater than  $S$  per steradian ( $10^2$ ,  $10^3$ ,  $10^4$  from bottom to top) with  $S = 10^{-13}$  erg cm $^{-2}$  s $^{-1}$  in the hard X-ray (2-10 keV) band and with  $S_\nu = 50$  mJy in the submm (0.85 mm) band, respectively. Thick dashed lines represent the *COBE* 4 year result computed from the fitting formulae at  $0.2 < \Omega_0 \leq 1$  by Bunn & White (1997).

data, however, we simply intend to perform a crude comparison with our predictions in Fig. 5.

The sky coverage of the XBACs is hard to quantify mainly due to the uncertain volume incompleteness of the underlying optical catalogue as noted by Ebeling et al. (1996). In Fig. 5, therefore, we simply plot the real numbers of the XBACs and normalize all our model predictions to match the total number of the XBACs at its flux limit  $S(0.1-2.4 \text{ keV}) = 5 \times 10^{-12}$  erg cm $^{-2}$  s $^{-1}$  and redshift limit  $z = 0.2$ . In general, the model predictions are shown to be capable of reproducing well the shape and amplitude of the observed distributions  $N(> S, > T, < z)$  even when  $T$  and  $z$  are varied. Taking into account the incompleteness of the observed data and large statistical fluctuations at low numbers, the agreements with models L03 and L03 $\gamma$  (both has  $\Omega_0 = 0.3$ ) are rather remarkable. Since the shapes and amplitudes of the predicted curves in these figures are primarily

determined by the value of  $\Omega_0$ , this result provides a further indication for low  $\Omega_0$  universe.

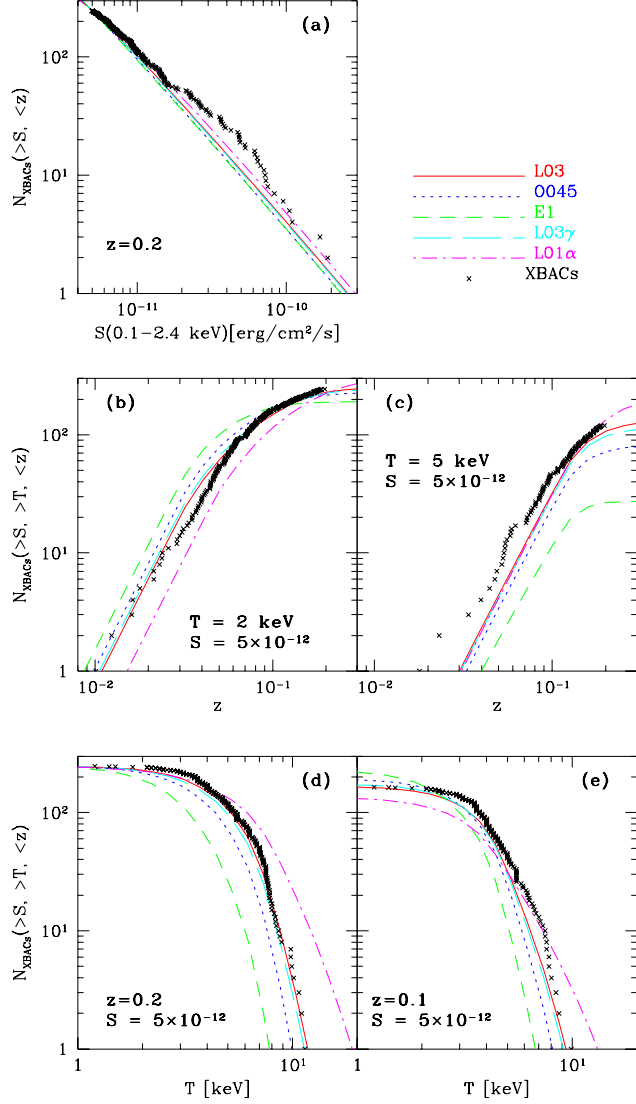


Figure 5. Tentative comparison with the XBACs (Ebeling et al. 1996). Upper panel (a) shows the LogN-LogS in the 0.1-2.4 keV band with the redshift limit of  $z = 0.2$  (models L03 and O045 almost overlap with L03 $\gamma$  and E1 respectively). Middle panels exhibit  $N(>S, >T, <z)$  versus  $z$  for  $S(0.1-2.4 \text{ keV}) = 5 \times 10^{-12} \text{ erg cm}^{-2} \text{ s}^{-1}$  in the cases of (b)  $T = 2 \text{ keV}$  and (c)  $T = 5 \text{ keV}$ . Lower panels plot  $N(>S, >T, <z)$  versus  $T$  for  $S(0.1-2.4 \text{ keV}) = 5 \times 10^{-12} \text{ erg cm}^{-2} \text{ s}^{-1}$  in the cases of (d)  $z = 0.2$  and (e)  $z = 0.1$ . All the model predictions are normalized to reproduce the total number of the XBACs at its flux limit  $S(0.1-2.4 \text{ keV}) = 5 \times 10^{-12} \text{ erg cm}^{-2} \text{ s}^{-1}$  and redshift limit  $z = 0.2$ .

#### 4. Summary

Let us summarize the conclusions of the present talk.

- (1) There exist several theoretical models which successfully reproduce the observed  $\text{Log}N\text{--Log}S$  relation of galaxy clusters over almost four orders of magnitude in X-ray flux.
- (2) The resulting  $\sigma_8$  is given by the following empirical fit (95% confidence limit):

$$\sigma_8 = (0.54 \pm 0.02 \pm 0.1) \times \Omega_0^{-0.35-0.80\Omega_0+0.55\Omega_0^2} \quad (5)$$

for  $\lambda_0 = 1 - \Omega_0$  CDM, and

$$\sigma_8 = (0.54 \pm 0.02 \pm 0.1) \times \Omega_0^{-0.28-0.91\Omega_0+0.68\Omega_0^2} \quad (6)$$

for  $\lambda_0 = 0$  CDM.

- (3) Low-density CDM models ( $n = 1$ ) with  $(\Omega_0, \lambda_0, h, \sigma_8) = (0.3, 0.7, 0.7, 1)$  and  $(0.45, 0, 0.7, 0.8)$  simultaneously account for the cluster  $\text{Log}N\text{--Log}S$ , XTF, the *COBE* 4 year normalization.

Maybe the most important point is that many cosmological models are more or less successful in reproducing the structure at redshift  $z \sim 0$  *by construction*. This is because the models have still several degrees of freedom or *cosmological parameters* which can be appropriately *adjusted* to the observations at  $z \sim 0$  ( $\Omega_0, \sigma_8, h, \lambda_0, b(r, z)$ ). We have shown that, given a complete flux limited cluster sample with redshift and/or temperature information, one can further constrain the cosmological models. In fact, our tentative comparison indicates that our predictions reproduce well the evolutionary features of the XBACs and that the results, although preliminary, seem to favor low density ( $\Omega_0 \sim 0.3$ ) universes. As indicated by this preliminary result, surveys of objects at high redshifts in several different bands (X-ray, radio and submm) are the most efficient and rewarding to break the degeneracy among the viable cosmological models.

**Acknowledgments.** We thank H. Ebeling and P. Rosati for generously providing us their X-ray data, and K. Masai for making his X-ray code available to us. Numerical computations presented here were carried out on VPP300/16R and VX/4R at the Astronomical Data Analysis Center of the National Astronomical Observatory, Japan, as well as at RESCEU (Research Center for the Early Universe, University of Tokyo) and KEK (National Laboratory for High Energy Physics, Japan). T.K. acknowledges support from a JSPS (Japan Society for the Promotion of Science) fellowship (09-7408). This research was supported in part by the Grants-in-Aid by the Ministry of Education, Science, Sports and Culture of Japan (07CE2002) to RESCEU, and by the Supercomputer Project (No.97-22) of High Energy Accelerator Research Organization (KEK).



## References

- Bahcall, N.A. & Cen, R.Y. 1993, ApJ 407 L49
- Barbosa, D., Bartlett, J. G., Blanchard, A., & Oukbir, J. 1996, A&A 314, 13
- Bunn, E. F., & White, M. 1997, ApJ 480, 6
- Cagnoni, I., Della Ceca, R., & Maccacaro, T. 1997, astro-ph/9709018
- David, L. P., Slyz, A., Jones, C., Forman, W., & Vrtillek, S. D. 1993, ApJ 412, 479
- Ebeling H., et al. 1998, MNRAS submitted
- Eke, V. R., Cole, S., & Frenk, C. S. 1996, MNRAS 282, 263
- Evrard, A.E., & Henry, J. P. 1991, ApJ 383, 95
- Fan, X., Bahcall, N.A. & Cen, R.Y. 1997, ApJ 490 L123
- Henry, J. P., & Arnaud, K. A. 1991, ApJ 372, 410
- Kitayama, T., Sasaki, S., & Suto, Y. 1998, PASJ 50, 1
- Kitayama, T., & Suto, Y. 1996a, MNRAS 280, 638
- Kitayama, T., & Suto, Y. 1996b, ApJ 469, 480
- Kitayama, T., & Suto, Y. 1997, ApJ 490, 557
- Lacey, C. G., & Cole, S. 1993, MNRAS 262, 627
- Masai, K. 1984, Ap&SS 98, 367
- Mushotzky, R.F., Scharf, C. A. 1997, ApJ 482, L13
- Oukbir, J., Bartlett, J. G., & Blanchard, A. 1997, A&A 320, 365
- Oukbir, J., & Blanchard, A. 1997, A&A 317, 10
- Pen, U. 1996, astro-ph/9610147
- Piccinotti, G., Mushotzky, R. F., Boldt, E. A., Holt, S. S., Marshall, F. E., Serlemitsos, P. J., & Shafer, R. A. 1982, ApJ 253, 485
- Press, W. H., & Schechter, P. 1974, ApJ 187, 425 (PS)
- Ponman, T. J., Bourner, P. D. J., Ebeling, H., & Böhringer, H. 1996, MNRAS 283, 690
- Rosati, P., & Della Ceca, R. 1997, in preparation
- Rosati, P., Della Ceca, R., Burg R., Norman, C., & Giacconi, R. 1995, ApJ 445, L11
- Rosati, P., Della Ceca, R., Norman, C., & Giacconi, R. 1997, ApJL submitted
- Sasaki, S. 1994, PASJ 46, 427
- Shimasaku, K. 1993, ApJ 413 59
- Sunyaev R.A., & Zel'dovich Ya.B. 1972, Commts. Astrophys. Space Phys. 4, 173
- Ueda, H., Itoh, M., & Suto, Y. 1993, ApJ 408 3
- Ueda, H., Shimasaku, K., Sugihara, T., & Suto, Y. 1994, PASJ, 46 319
- Viana, P. T. P., & Liddle, A. R. 1996, MNRAS 281, 323
- White, S. D. M., Efstathiou, G., & Frenk, C. S. 1993, MNRAS 262, 1023